

Time- and Space-Resolved Study of a Dressed Polariton: The Polariton Fermi Resonance in Ammonium Chloride

F. Vallée, G. M. Gale, and C. Flytzanis

Laboratoire d'Optique Quantique du Centre National de la Recherche Scientifique, Ecole Polytechnique, 91128 Palaiseau CEDEX, France

(Received 8 June 1988)

Using a time- and space-resolved coherent anti-Stokes Raman-scattering technique we study the dephasing of a polariton state that crosses and strongly couples with a two-phonon band. Polariton damping is found to be dominated by a direct and phonon-assisted disintegration of the polariton into the two-phonon continuum.

PACS numbers: 42.65.Dr, 42.65.Re, 78.47.+p

The polariton Fermi resonance is a very conspicuous feature of polariton-mode propagation in crystals. It is produced whenever a polariton branch crosses a many-phonon band, most often two phonon, of the same symmetry as the polariton.¹ This situation is frequently encountered because both polariton and two-phonon states span large regions in frequency and wave-vector space. For sufficiently strong anharmonic coupling, polariton Fermi resonance leads to a drastic alteration of polariton characteristics, formation of an additional gap in the polariton dispersion curve, and strong, frequency-dependent damping of the polariton line.^{1,2} The otherwise slowly moving two-phonon states are also affected, acquiring polaritonlike properties.

Polariton dispersion and the new gap formation have been extensively studied in several crystals with use of spontaneous near-forward Raman or hyper-Raman techniques.^{1,2} The severe modification of polariton relaxation that occurs in the vicinity of a many-phonon band is, however, very difficult to address with these or similar local nonlinear optical techniques, whether in the frequency or time domain. This difficulty arises because of the large variation of polariton frequency with scattering angle and related propagation effects. Furthermore, for these fast-moving composite excitations, relaxation, and propagation effects affect their coherence and energy content on comparable time scales, and adequate methods must be devised to disentangle these processes. Although femtosecond far-infrared pulses have been used to perform coherent time-domain spectroscopy of infrared and Raman-active modes,³ this method is restricted to low-frequency polaritons, with an upper frequency limit given by the infrared femtosecond pulse bandwidth. However, for Raman-active polariton modes it has been shown recently that a nonlocal technique, namely, time- and space-resolved coherent anti-Stokes Raman scattering (CARS),⁴ allows the proper separation of temporal and spatial features, while placing no restriction on polariton frequency.

We have performed the first time- and space-resolved study of polariton Fermi resonance in ammonium

chloride (NH₄Cl), in a frequency region where the polariton is in strong interaction with the polar (2ν₄) two-phonon band,^{5,6} which extends⁷ roughly from 2800 to 2900 cm⁻¹ (see Fig. 1). We focus our attention on the damping mechanisms that affect this composite mode, its dispersion curve and Raman spectrum having been extensively studied by conventional techniques.^{5,8}

Within the formalism of Green's functions the polariton Fermi resonance, or dressed polariton, is defined by the propagator $G_p(\omega, k)$ which is related to the bare polariton propagator $G_p^0(\omega, k)$ through the Dyson equation,⁹

$$G_p(\omega, k) = G_p^0(\omega, k) \{1 - X^2(k) G_p^0(\omega, k) g_2(\omega, k)\}^{-1}, \quad (1)$$

where

$$G_p^0(\omega, k) = \{\omega - \omega_p^0(k) + i\gamma_p/2\}^{-1}. \quad (2)$$

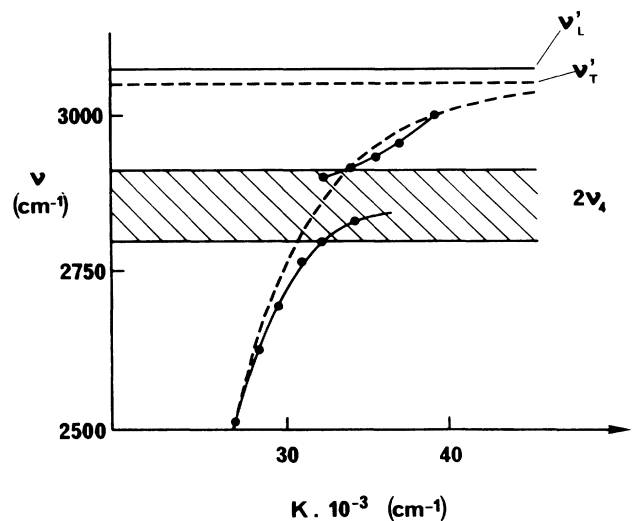


FIG. 1. The polariton dispersion curve of ammonium chloride in the vicinity of the 2ν₄ two-phonon quasicontinuum (shaded region) obtained by near-forward Raman scattering (filled circles) (Ref. 5). The dashed curve is the calculated dispersion curve in the absence of polariton Fermi resonance.

$\omega_p^0(k)$ and γ_p are, respectively, the polariton dispersion law and damping rate in the absence of Fermi resonance, and $g_2(\omega, k)$ is the two-phonon propagator with anharmonicity included (ν_4 intramolecular anharmonicity in our case). The polariton-two-phonon anharmonic coupling X is composed¹⁰ of a mechanical part X_M and an electro-optic part X_E but, supposing the latter to be negligible, we may write^{1,2}

$$X^2(k) = X_M^2 S(k), \quad (3)$$

where $S(k)$ is the fraction of mechanical energy in the bare polariton of wave vector k . Similarly,¹¹

$$\gamma_p = \gamma_p^0 S(k), \quad (4)$$

for the bare polariton damping where γ_p^0 may depend on frequency in general.^{4,12}

The polariton density of states defined by $\rho(\omega, k) = -(1/\pi)\text{Im}G_p(\omega, k)$ is

$$\rho(\omega, k) = \frac{\pi X^2(k) \rho_2(\omega, k) + \gamma_p/2}{[\omega - \omega_p^0(k) - X^2(k) \text{Re}g_2(\omega, k)]^2 + [\pi X^2(k) \rho_2(\omega, k) + \gamma_p/2]^2}, \quad (5)$$

with $\rho_2(\omega, k) = -(1/\pi)\text{Im}g_2(\omega, k)$ the anharmonic two-phonon density of states. Compared with the bare polariton [Eq. (2)] the dressed polariton [with Fermi resonance, Eq. (1)] has a new dispersion law given¹ by the maximum of Eq. (5), and a quasi-Lorentzian line shape with a width

$$\gamma_p(k_p) = \gamma_p + 2\pi X^2(k_p) \rho_2(\omega_p, k_p) = [\gamma_p^0 + 2\pi X_M^2 \rho_2(\omega_p, k_p)] S(k_p). \quad (6)$$

The second term in (6), which is proportional to the two-phonon density of states, is due to the direct polariton-two-phonon interaction and leads to a dramatic modification of polariton line broadening in the neighborhood of a two-phonon band. It is this term which is the principal object of the present investigation using the time- and space-resolved CARS technique.

As the essence of this technique has already been described elsewhere, and demonstrated on the ν_4 polariton of ammonium chloride,^{4,13} we simply recall here that a picosecond-duration polariton wave packet of frequency ω_p is created at an initial instant and space point in the crystal by coherent Raman scattering using time-coincident picosecond pulses of frequencies ω_L and ω_S , such that $\omega_L - \omega_S = \omega_p$. This polariton wave packet subsequently propagates freely inside the crystal in a direction fixed by overall wave-vector conservation, and its temporal and spatial evolution is followed by coherent anti-Stokes Raman scattering of a picosecond probe pulse (ω_{pr}) displaced in time and space with respect to the excitation. The measured dependence between probing position and optimum-signal probe time delay gives direct access to polariton group velocity, and the variation of coherent signal intensity with probe time (and space) delay yields⁴ polariton dephasing times T_2 . The three independent picosecond pulses necessary for the experiment, ω_{pr} , ω_S , and ω_L , which is continuously tunable, are produced by frequency conversion of a single 5-ps infrared pulse provided by a passively mode-locked Nd³⁺:glass laser. The three beams are focused into a cooled 10-mm-long NH₄Cl crystal with use of a noncollinear geometry and the generated anti-Stokes signal is detected after suitable filtering.

Figure 2 shows a plot of the observed coherent anti-Stokes signal as a function of probe delay, for a polariton frequency of $\nu_p = 2740 \text{ cm}^{-1}$ and a crystal temperature of 78 K. Note that probe time delay and spatial position were varied simultaneously to "follow" the polariton in-

side the crystal. After a rapid rise, the coherent signal decays exponentially over nearly 7 orders of magnitude, yielding $T_2 = 7.7 \pm 0.8 \text{ ps}$ for this polariton frequency at 78 K. Exponential decay is observed for all polariton frequencies studied, including inside the $2\nu_4$ two-phonon band, indicating a Lorentzian polariton line shape throughout this range. The linewidth and amplitude (scattering cross section) of these Lorentzians depend markedly on polariton frequency, however, implying that mixing of the bare polariton and two-phonon states opens new relaxation channels and leads to a strong

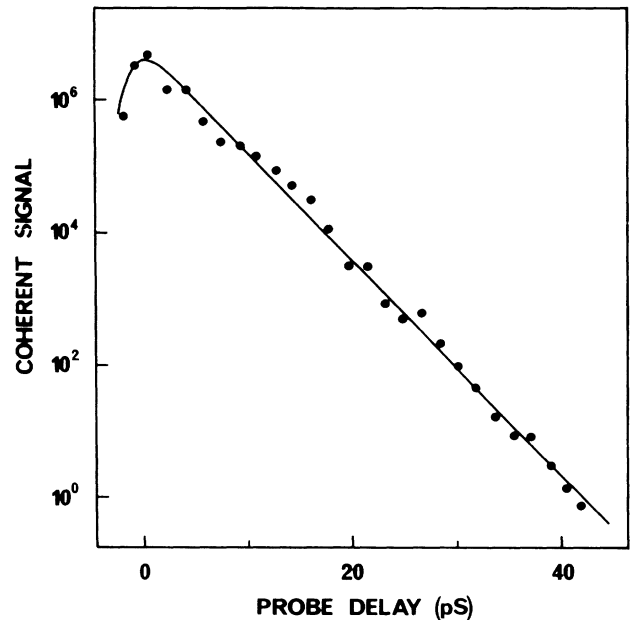


FIG. 2. Space- and time-resolved CARS signal from the 2740-cm^{-1} "followed" polariton in NH₄Cl at 78 K, plotted on a logarithmic scale as a function of probe delay (t_D).

redistribution of oscillator strength between the various branches.^{1,2}

The dramatic frequency dependence of the dephasing rate $2/T_2 = 2\pi\Gamma_p(\nu_p)$ is depicted in Fig. 3 for a fixed crystal temperature of 78 K and various polariton frequencies close to the edges of the $2\nu_4$ band. The very rapid increase of Γ_p inside the $2\nu_4$ band is a clear indication that the isoenergetic two-phonon states provide a direct and very efficient polariton relaxation channel. This means, in particular, that the second term in (6) is dominant inside the $2\nu_4$ continuum and thus the measured Γ_p essentially reflects the two-phonon density of states which, by definition, increases rapidly at the edges of the two-phonon band.

Outside the two-phonon continuum, this relaxation mechanism is not directly accessible and damping is determined by the channels incorporated in the first term of (6). Polaritons close to the two-phonon band edges may still preferentially relax into this band with the assistance of low-energy lattice phonons of frequency ν_E , in an up- or down-conversion process. If we single out this mechanism, introducing energy and momentum conservations, the coefficient γ_p can be written $\gamma_+^0 + S\Gamma_{2\nu_4}[1 + n(\nu_E)]$ above the two-phonon continuum (down-conversion process) and $\gamma_-^0 + S\Gamma_{2\nu_4}n(\nu_E)$ below it (up-conversion process), where $n(\nu_E)$ is the low-energy phonon occupation number and $\Gamma_{2\nu_4}$ is an anharmonic coupling coefficient which can be taken as frequency independent in the frequency range studied. Apart from the difference due to the different nature of the processes above and below the two-phonon band (down and up conversion) the frequency dependence is embodied mainly in the polariton phonon-strength factor $S(k_p)$ and to a lesser extent in the small residual damping constants γ_+^0 and γ_-^0 . These latter residual constants may be different

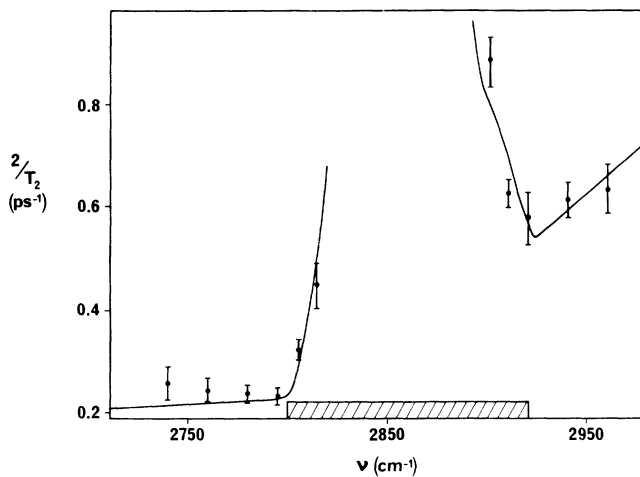


FIG. 3. Measured polariton dephasing rate $2/T_2$ ps⁻¹ vs polariton frequency, under conditions of Fermi resonance with the $2\nu_4$ band (shaded region), at a crystal temperature of 78 K. The full line is calculated (see text).

because of the presence of additional higher-order many-phonon bands which, because of energy and momentum conservation restrictions, may intervene differently above and below the $2\nu_4$ continuum.

On the basis of these assumptions, the overall damping rate of the dressed polariton may be represented by

$$\Gamma_p = \gamma_-^0 + \{\Gamma_{2\nu_4}^0 n(\nu_E) + 2\pi X_M^2 \rho_{2\nu_4}(\nu_p)\} S(k_p), \quad (7)$$

close to the lower edge of the $2\nu_4$ band and,

$$\Gamma_p = \gamma_+^0 + \{\Gamma_{2\nu_4}^0 [1 + n(\nu_E)] + 2\pi X_M^2 \rho_{2\nu_4}(\nu_p)\} S(k_p), \quad (8)$$

near the upper limit of the two-phonon band.

Taking into account lattice phonon density of states¹⁴ and energy conservation restrictions allows us to use a mean value of ν_E of 90 cm⁻¹. The two-phonon density of states $\rho_{2\nu_4}(\nu_p)$ was estimated from the F_2 -symmetry 90° spontaneous Raman spectrum,^{7,8,15} and γ_-^0 is obtained from low-temperature (<10 K) measurements well outside the two-phonon continuum. Because of the $(1+n)$ factor in (8), γ_+^0 cannot be obtained in this way. The overall behavior of Γ_p is very well reproduced (full line in Fig. 3) with $\gamma_-^0 = 0.15$ cm⁻¹, $\Gamma_{2\nu_4} = 3.8$ cm⁻¹, $X_M = 15$ cm⁻¹, and $\gamma_+^0 \approx 0.0$ cm⁻¹ with an uncertainty of roughly 0.2 cm⁻¹ in the latter value. One might expect a larger value for γ_-^0 than for γ_+^0 because the polariton crosses an infrared-active higher-order many-phonon band lying below the $2\nu_4$ continuum^{6,16} into which it may decay. This does not occur above the two-phonon band.

The detailed relaxation processes outlined above for the dressed polariton receive additional support from our temperature-dependent measurements of the polariton dephasing rate, as exemplified in Fig. 4. Indeed, very good agreement with the temperature variations predicted by expressions (7) and (8) is obtained over the whole frequency range studied and for temperatures ranging from 10 to 120 K. At higher temperatures, additional phonon-assisted up-conversion processes into other continua may become important,¹³ as well as dephasing of the electromagnetic part of the polariton by the crystal disorder that is introduced as the phase transition of ammonium chloride at 243 K is approached.⁴

In conclusion, we have shown that time- and space-resolved CARS is well adapted to the investigation of polariton-many-phonon interactions in noncentrosymmetric crystals and that this technique gives, for the first time, direct access to polariton dephasing under the conditions of polariton Fermi resonance. Our frequency- and temperature-dependent measurements demonstrate clearly the critical role played by the two-phonon band in polariton damping, not only through the direct decay of degenerate polaritons into two phonons, but also via an indirect lattice-phonon-assisted process for polaritons outside the two-phonon continuum. These processes are similar to those observed for two-phonon bound

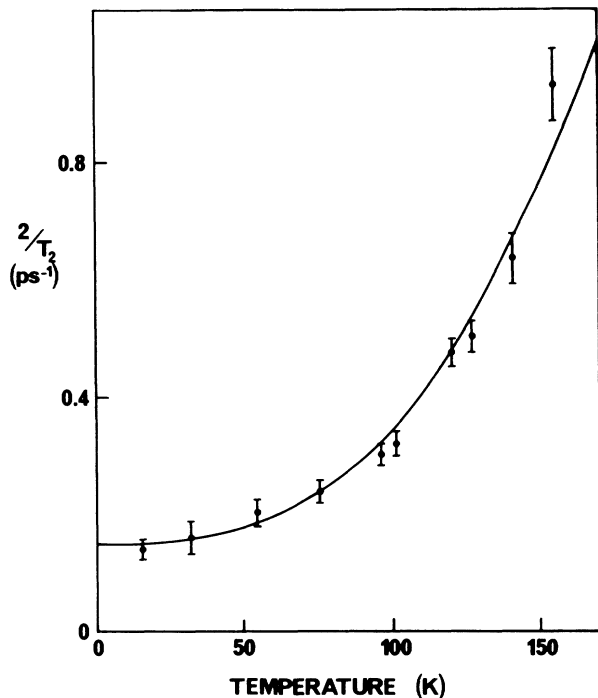


FIG. 4. Temperature dependence of the damping rate of the 2780-cm^{-1} polariton which lies just below the $2\nu_4$ two-phonon continuum. The curve is calculated (see text).

states.^{17,18}

Furthermore, our technique constitutes a powerful and almost unique tool for the continuous probing of crystal anharmonicity as a function of frequency, which, together with temperature-dependent measurements, opens up new possibilities for the investigation of anharmonic processes in solids. This technique could be applied to the study of many other kinds of interactions in crystals such as polariton-defect or polariton-impurity coupling. Specifically, the observation of polariton dynamics in a crys-

tal with an arbitrary concentration of impurity could be particularly interesting.

¹V. M. Agranovich and I. I. Lalov, *Usp. Fiz. Nauk.* **146**, 267 (1985) [*Sov. Phys. Usp.* **28**, 484 (1985)].

²V. N. Denisov, B. N. Mavrin, V. B. Podobedov, and K. E. Sterin, *Zh. Eksp. Teor. Fiz.* **82**, 406 (1982) [*Sov. Phys. JETP* **55**, 232 (1982)].

³D. H. Auston and M. C. Nuss, *IEEE J. Quantum Electron.* **24**, 184 (1988).

⁴G. M. Gale, F. Vallée, and C. Flytzanis, *Phys. Rev. Lett.* **57**, 1867 (1986).

⁵G. G. Mitin, V. S. Gorelik, L. A. Kulevskii, Y. N. Pivivanov, and M. M. Sushchinskii, *Zh. Eksp. Teor. Fiz.* **68**, 1757 (1975) [*Sov. Phys. JETP* **41**, 882 (1975)].

⁶V. S. Gorelik, O. P. Maximov, G. G. Mitin, and M. M. Sushchinskii, *Solid State Commun.* **21**, 615 (1977).

⁷G. G. Mitin, V. S. Gorelik, and M. M. Sushchinskii, *Fiz. Tverd. Tela (Leningrad)* **16**, 2956 (1974) [*Sov. Phys. Solid State* **16**, 1912 (1975)].

⁸L. R. Fredrickson and J. C. Decius, *J. Chem. Phys.* **66**, 2297 (1977).

⁹A. A. Anikiev, L. C. Reznik, B. S. Umarov, and J. F. Scott, *J. Raman Spectrosc.* **15**, 60 (1984).

¹⁰I. I. Lalov and K. T. Stoychev, *Bulg. J. Phys.* **6**, 304 (1979).

¹¹R. Loudon, *J. Phys. A* **3**, 233 (1970).

¹²S. Ushioda, J. D. McMullen, and M. J. Delaney, *Phys. Rev. B* **8**, 4634 (1973).

¹³G. M. Gale, F. Vallée, and C. Flytzanis, to be published.

¹⁴C. H. Kim, H. A. Rafizadeh, and S. Yip, *J. Chem. Phys.* **57**, 2291 (1972).

¹⁵M. V. Belousov and D. E. Pogarev, *Pis'ma Zh. Eksp. Teor. Fiz.* **28**, 692 (1978) [*JETP Lett.* **28**, 644 (1978)].

¹⁶N. E. Schumaker and C. W. Garland, *J. Chem. Phys.* **53**, 392 (1970).

¹⁷F. Bogani, G. Cardini, V. Schettino, and P. L. Tasselli, in *Dynamics of Molecular Crystals*, edited by J. Lascombe (Elsevier, New York, 1987).

¹⁸F. Vallée, G. M. Gale, and C. Flytzanis, *Chem. Phys. Lett.* **149**, 572 (1988).